

## FORMULATION EVALUATION

### 7.1 Introduction:

The *in-vitro* and in-silico evaluation of optimized formulations was performed to study the desired characteristics using various techniques enlisted below in table 7-1.

Table 7-1 List of evaluation techniques for optimized formulation

Sr. No.	Evaluation technique	Intended use
1	% Yield calculation	Desirability of manufacturing process
2	Fourier transform Infrared (FTIR) spectroscopy	Interaction of active pharmaceutical ingredient with excipients and localization of drug within formulation matrix.
3	Thermal analysis using differential scanning calorimetry (DSC)	Thermotropic behaviour of optimized formulations. Interaction of active pharmaceutical ingredient with excipients and localization of drug within formulation matrix.
4	Particle size analysis by Malvern	Particle size distribution of formulations
5	Morphology by optical microscopy	External morphology and Particle size
6	Morphology by Scanning electron microscopy	External morphology, surface characteristics, particle size
7	Estimation of drug loading and entrapment efficiency	Estimation of drug content and loading capacity
8	Micromeritics	Flow properties of microspheres
9	<i>In-vitro</i> drug release studies: Accelerated method	Estimation of drug release in quick time for decision making
10	<i>In-vitro</i> drug release studies: Real time method	Estimation of drug release in real time mimicking desired <i>in-vivo</i> duration
11	<i>In-vitro</i> drug release studies: Biorelevant method	Estimation of drug release in real time mimicking desired <i>in-vivo</i> environment and duration
12	Drug release kinetics	Understand mechanism of drug release
13	Stability studies	Assessment of storage conditions on CQAs and determination of shelf life
14	Haemolysis studies	Compatibility of formulations post injection with physiological environment and toxicity of formulations to blood components
15	In-silico PBPK model	Prediction of <i>in-vivo</i> pharmacokinetics
16	Virtual bioequivalence studies	Bioequivalence with reference formulation
17	<i>In-vitro In-vivo</i> correlation	Establishment of <i>in-vivo</i> design space

## 7.2 *In-vitro* characterization studies:

### 7.2.1 Determination of Yield:

The manufacturing yield of Janus microspheres of optimized formulations was calculated by as per the equation 7-1.

$$\% \text{ yield} = \frac{\text{Actual yield}}{\text{Theoretical yield}} \times 100 \dots \dots \dots (7-1)$$

Percentage yield was found to be  $80 \pm 10 \%$  for the optimized formulations.

### 7.2.2 FTIR analysis:

Optimized formulation was analyzed using FTIR method described previously and FTIR spectrum is presented in Figure 7-1.

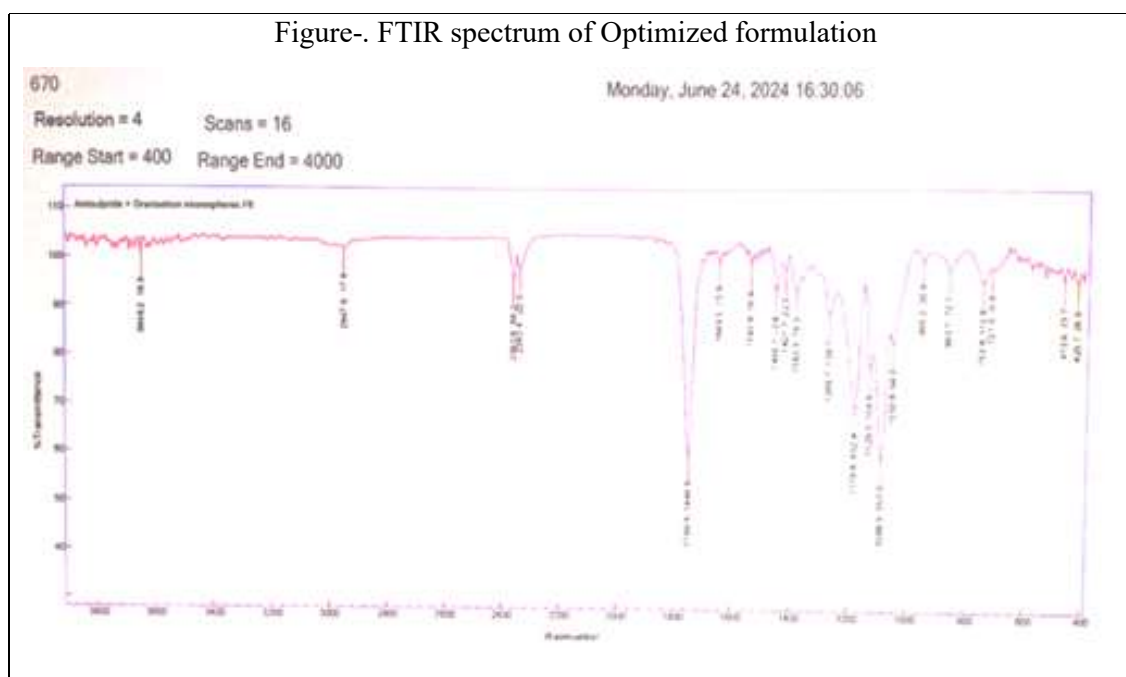


Figure 7-1 FTIR spectrum of Optimized formulation

Formulation spectra showed the presence of only polymer (PLGA and PCL) peaks  $1749, 1455, 1382, 1270, 1179, 1129, 1088, 866$  and  $750 \text{ cm}^{-1}$  [1,2] suggesting complete encapsulation of drugs within the polymers at molecular level.

### 7.2.3 Thermal analysis by DSC:

Optimized formulation was analysed using differential scanning calorimetry (DSC) method described previously and thermogram is shown in Figure 7-2.

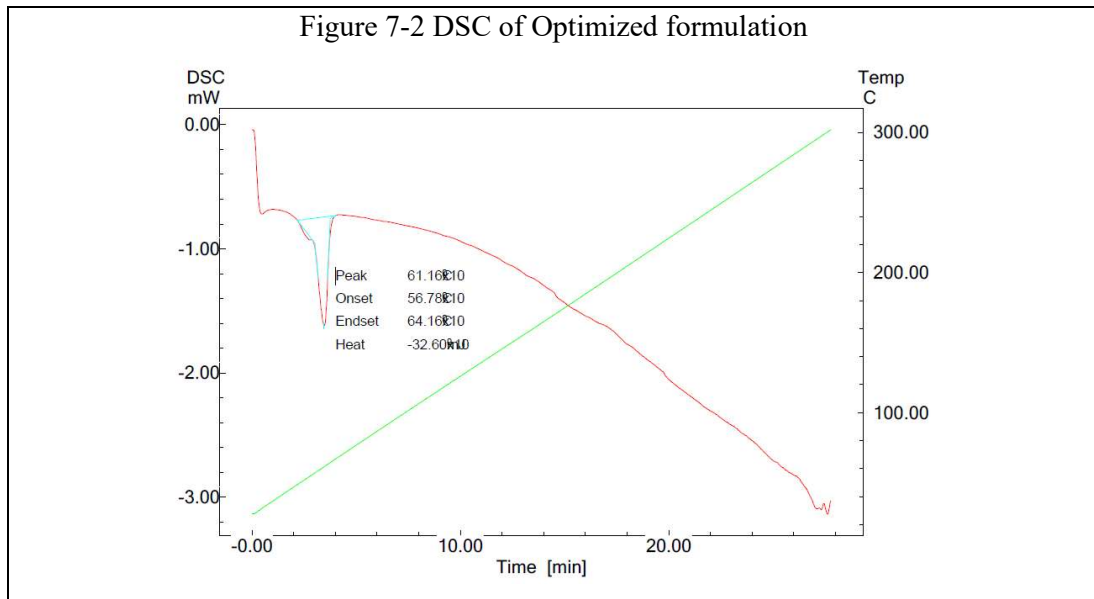


Figure 7-2 DSC of Optimized formulation

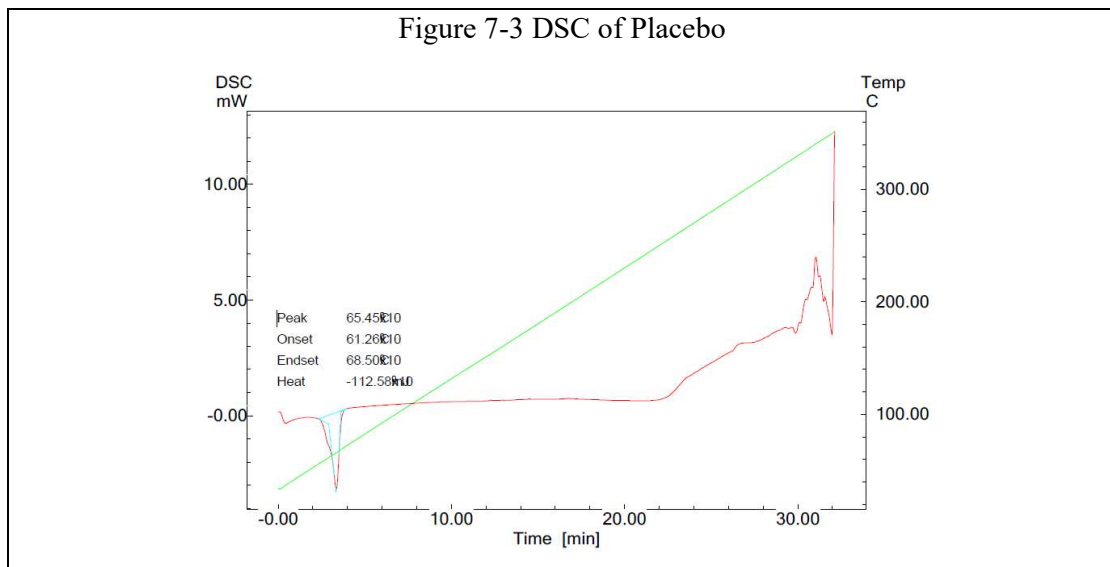


Figure 7-3 DSC of placebo

The absence of drug peaks (Amisulpride at 128.8°C and Granisetron at 301.36°C) [3, 4] and presence of only polymer (PLGA and PCL) peaks [5,6] confirms the complete encapsulation within the polymer. The formulation thermogram showed the fusion peak of the PCL and PLGA at 61.16°C [6]. The small shoulder peak corresponds to the PLGA glass transition temperature. The same phenomenon is also observed in placebo where the fusion peak and shoulder peak appeared at 65.45°C as shown in figure 7-3.

#### 7.2.4 Particle size analysis:

The particle size analysis was performed using Malvern 3000 (Malvern Instrument, Worcestershire, United Kingdom). Microspheres were suspended in 0.01% Tween 80 aqueous

solution and subjected to ultrasonic treatment for 10 seconds and particle size was measured using laser diffraction [7]. Optimized formulation showed particle size of around  $100 \pm 20$  microns which are suitable for intramuscular/subcutaneous injection. The particle size of optimized formulation is shown in figure 7-4 and table 7-2.

Table 7-2 Particle size distribution of Optimized Formulation

Formulation	Particle size distribution
Optimized formulation	D10: $35.789 \pm 2.95$
	D50: $60.181 \pm 3.97$
	D90: $92.181 \pm 3.66$

d(0.1) : 35.789  $\mu\text{m}$

d(0.5) : 60.181  $\mu\text{m}$

d(0.9) : 92.181  $\mu\text{m}$

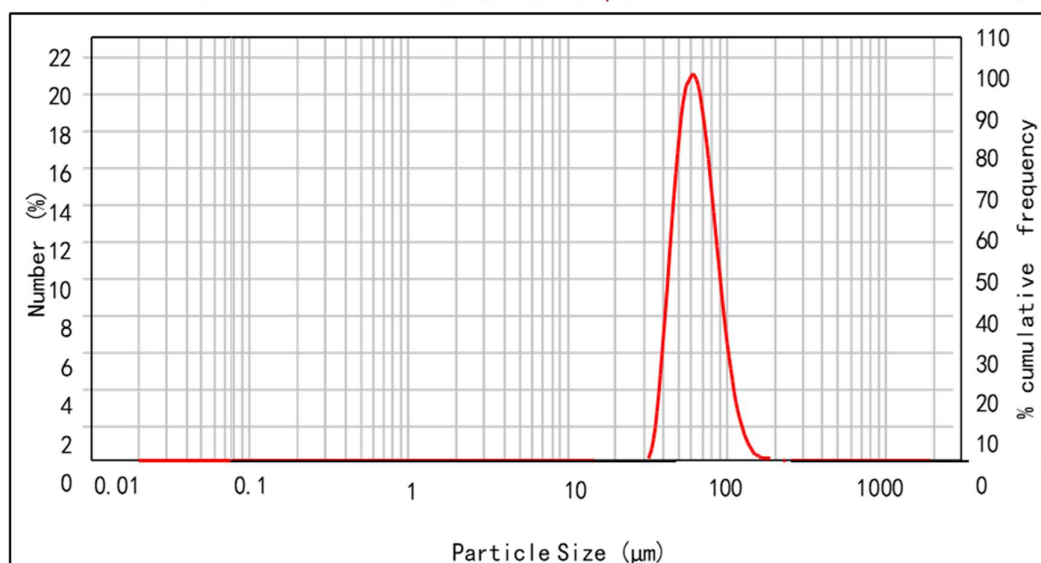


Figure 7-4 Particle size distribution of Optimized formulation

### 7.2.5 Morphology by optical microscopy:

The particle size and morphology were studied using optical microscopy. It was observed that, during preparation, dual drug loaded Janus microspheres have typical handbag like structure [8]. After drying, the particles appeared in more spherical shape as observed in Figure 7-5 E to 7-5H. When the W/O emulsion was added to external water phase containing 0.5% PVA, the formation of handbag like structure started appearing (Nascent stage) as can be seen in Figure 7-5 A to 7-5 D.

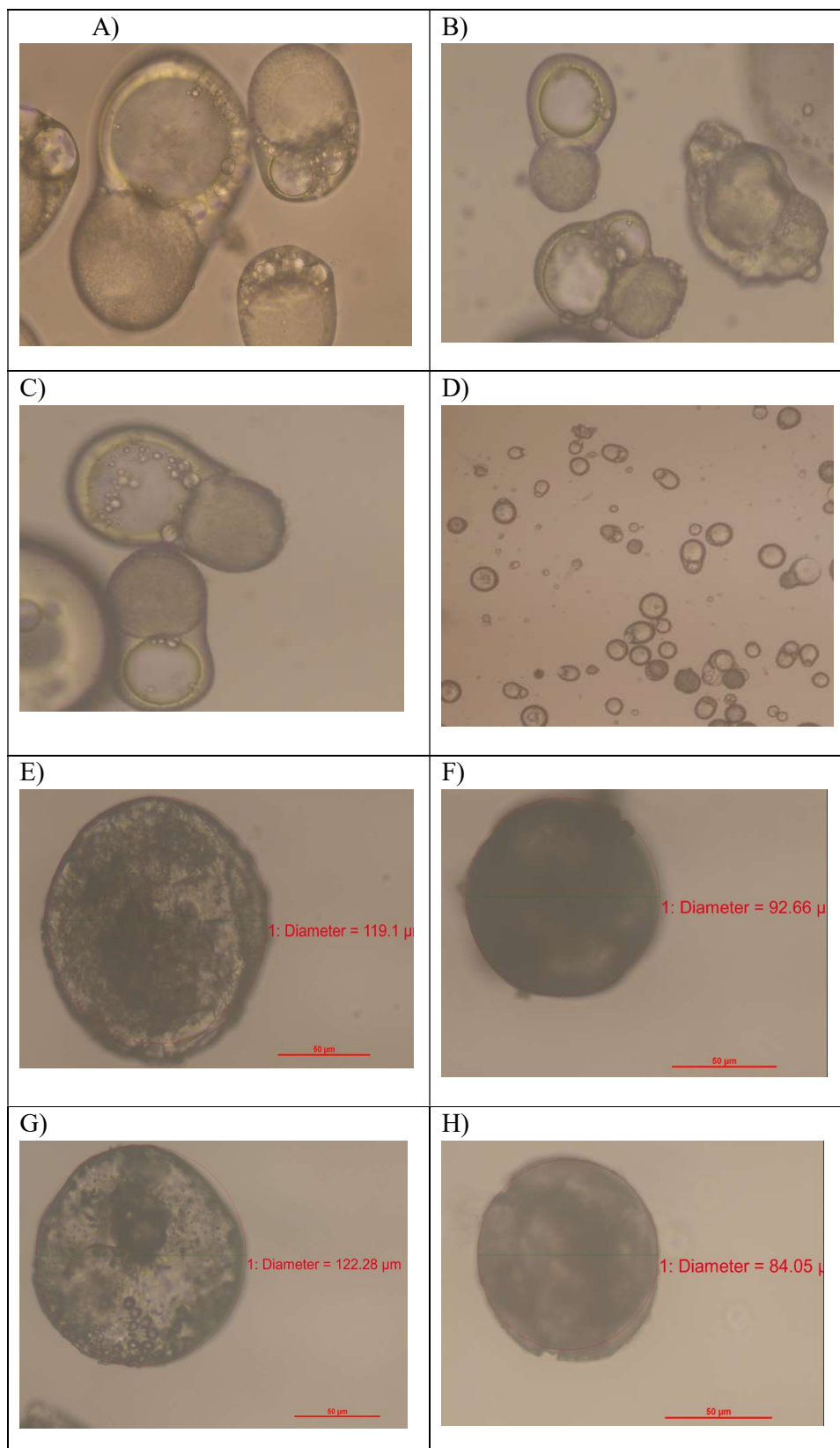
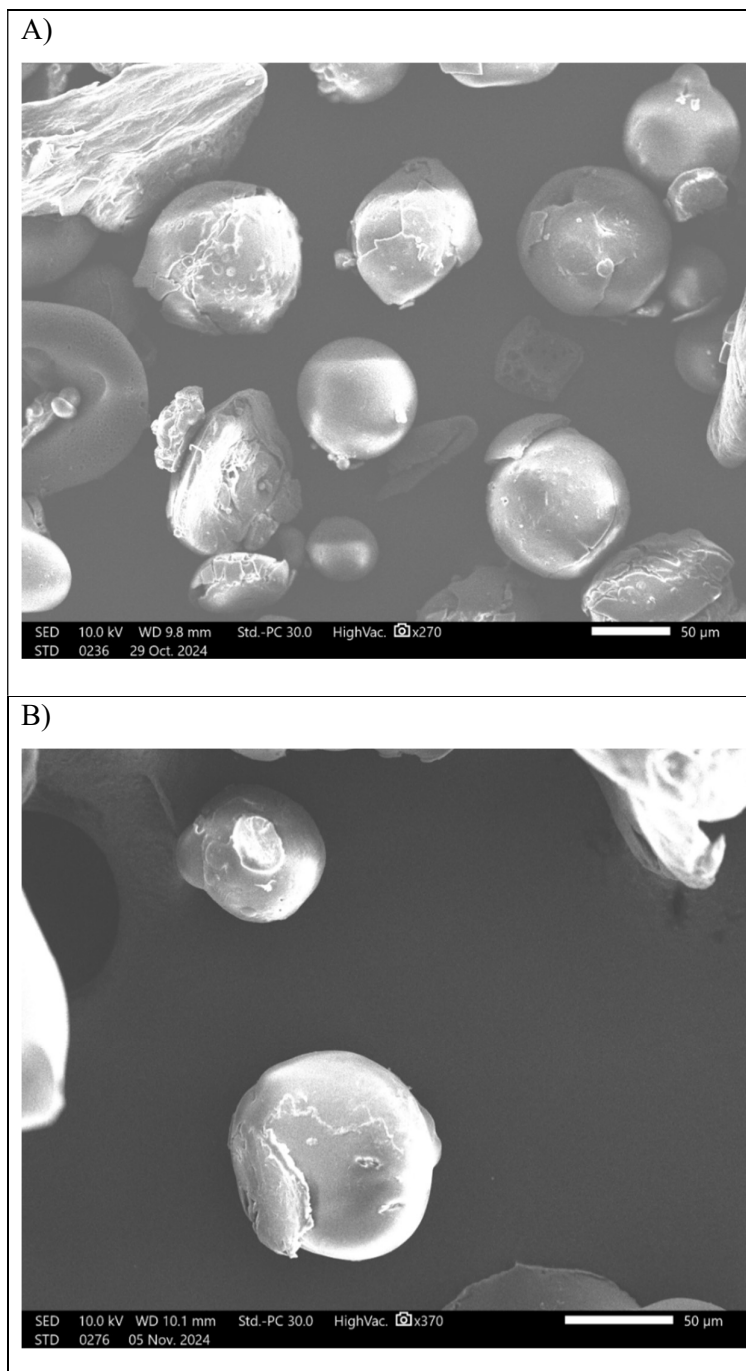


Figure 7-5 Optical microscopic images of optimized formulation A to D: Nascent Initial stage, E to H: After drying (Finished product)

**7.2.6 Morphology by Scanning electron microscopy:**

To study the morphology and surface characteristics of the prepared Janus microspheres, the particles were subjected to scanning electron microscopy (SEM). 1 mg of formulations were kept on sticky tape stucked on aluminium block. 20 KV AC voltage was used for measurement [9]. Electrical Research and Development Association (ERDA), Lucknow facility was used to take the measurements using SEM instrument-JSM-6380LV, JEOL. The SEM images of the optimized formulation are shown in figure 7-6 (A-C)



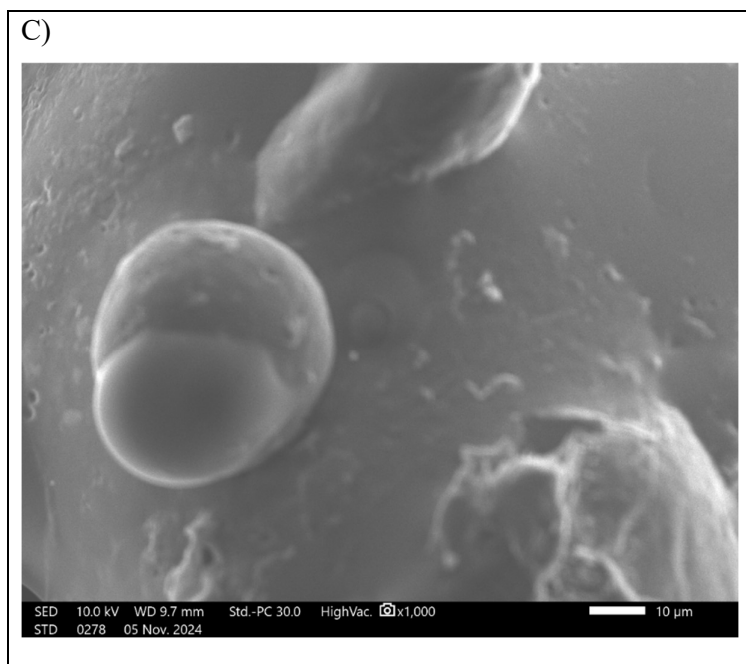


Figure 7- 6 Scanning microscopy images of optimized Formulation (A to C)

SEM images showed the formation of Janus microspheres with uniform particle size and morphology. The unique shape can be clearly visible in isolated microsphere in Fig 7-6C, where two compartments can be visibly observed.

### 7.2.7 Drug loading and Entrapment efficiency (%):

$$\%Drug\ loading = \frac{(Total\ drug - Free\ drug)\ in\ mg}{Weight\ of\ microspheres\ (mg)} \times 100$$

$$\%EE = \frac{Encapsulated\ drug\ (mg)}{Total\ amount\ of\ drug\ (mg)} \times 100$$

The % drug loading and % entrapment efficiency for optimized formulation are shown in table 7-3.

Table 7-3 Drug loading and Entrapment efficiency results for optimized formulation

Drug	% Drug Loading Average	SD	% Entrapment Efficiency	SD
Ami	14.08	0.38	65.69	1.75
Grani	4.76	0.17	66.67	2.41

### 7.2.8 Micromeritics:

The micromeritic studies for optimized formulation were carried out to measure flow properties [10]. Hausner's ratio for optimized formulation was found to be  $1.03 \pm 0.2$ , which indicates excellent flow properties [10].

**7.2.9 In-vitro Drug release studies:**

Drug release studies were carried out on optimized formulations. The drug release methods were selected based on literature and domain knowledge [11-14] The Accelerated method (ACC) helps to understand drug release behaviour in short period of time and avoid waiting for results till real time analysis. Pure API were also tested for drug release in same methods.

**A) Accelerated Method:**

Method used Liu Z et.al was modified and used. Briefly, formulation was placed in Eppendorf tubes containing pH 7.4 phosphate buffer saline. The tubes were kept in metabolic shaker operated at 100 rpm at temperature of 50°C. At each point of sampling, sample was centrifuged and analyzed for drug release [12]. Sampling was done on 1 hr, 4hr, 12hr and 24hr. Drug release was determined using HPLC. The results are shown in table 7-4, table 7-5 and figure 7-7. % RSD has been mentioned in bracket. The % RSD was higher at initial points due to lower release and subsequently improved as release increased.

Table 7-4 Drug release as per ACC IVRT method (Pure Drug)

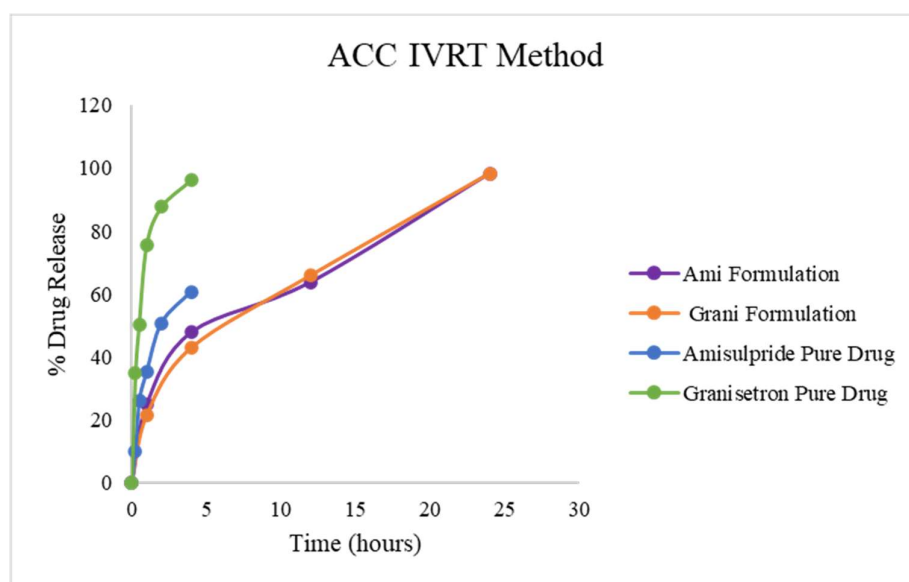
Accelerated <i>in-vitro</i> release testing method		
Time (hours)	Ami Pure Drug	Grani Pure Drug
0	0	0
0.25	10.1 (14.94)	34.7 (6.79)
0.5	25.8 (9.10)	50.3 (4.28)
1	35.1 (5.77)	75.5 (2.87)
2	50.7 (5.16)	87.7 (1.23)
4	60.7 (3.90)	96.2 (0.91)
24	70.6 (3.59)	97.1 (0.43)

Note: % RSD values provided for mean values in bracket

Table 7-5 Drug release as per ACC IVRT method (Formulation)

Accelerated <i>in-vitro</i> release testing method		
Time (hours)	Ami	Grani
0	0	0
1	24.9 (14.24)	21.4 (14.29)
4	47.8 (12.50)	42.9 (11.63)
12	63.9 (9.38)	65.9 (9.09)
24	98.4 (2.04)	98.3 (2.04)

Note: % RSD values provided for mean values in bracket

Figure 7-7 IVRT data from Accelerated *in-vitro* release testing method

The drug release using ACC method showed that, around 40-50% drug was released at 4-hour and almost complete release was observed at 24-hour.

### B) Real time method:

Method used Liu Z et.al was modified and used. Briefly, formulation was placed in Eppendorf tubes containing pH 7.4 phosphate buffer saline. The tubes were kept in metabolic shaker operated at 100 rpm at temperature of 37°C. At each point of sampling, sample was centrifuged and analyzed for drug release [12]. Sampling was done on 1 hr, 4hr, 12hr, 24hr, 48hr, 72hr, 96hr, 120hr, 144hr and 168 hr. Drug release was determined using HPLC. The results are shown in table 7-6, table 7-7 and figure 7-8. % RSD has been mentioned in bracket.

Table 7-6 Drug release as per real time IVRT method (Pure Drug)

Real time <i>in-vitro</i> release testing method		
Time (hours)	Ami Pure Drug	Grani Pure Drug
0	0	0
0.25	5.4 (18.44)	10.7 (14.14)
0.5	8.4 (14.92)	15.0 (6.70)
1	10.0 (14.06)	25.4 (4.84)
2	11.5 (10.05)	45.0 (4.02)
4	24.6 (7.93)	60.0 (3.77)
24	50.7 (4.41)	78.7 (1.80)

Note: % RSD values provided for mean values in bracket

Table 7-7 Drug release as per real time IVRT method (Formulation)

Real time <i>in-vitro</i> release testing method		
Time (hours)	Ami	Grani
0	0	0
1	15.6 (16.06)	1.9 (50.21)
4	19.1 (10.51)	7.9 (12.69)
12	26.6 (9.42)	22.9 (8.74)
24	43.9 (9.23)	41.1 (7.67)
48	62.9 (7.95)	65.9 (6.22)
72	84.3 (4.16)	81.1 (3.95)
96	92.9 (2.16)	89.1 (3.48)
120	92.9 (1.08)	94.1 (1.23)
144	96.9 (1.04)	95.9 (1.05)
168	98.6 (0.52)	97.9 (1.04)

Note: % RSD values provided for mean values in bracket

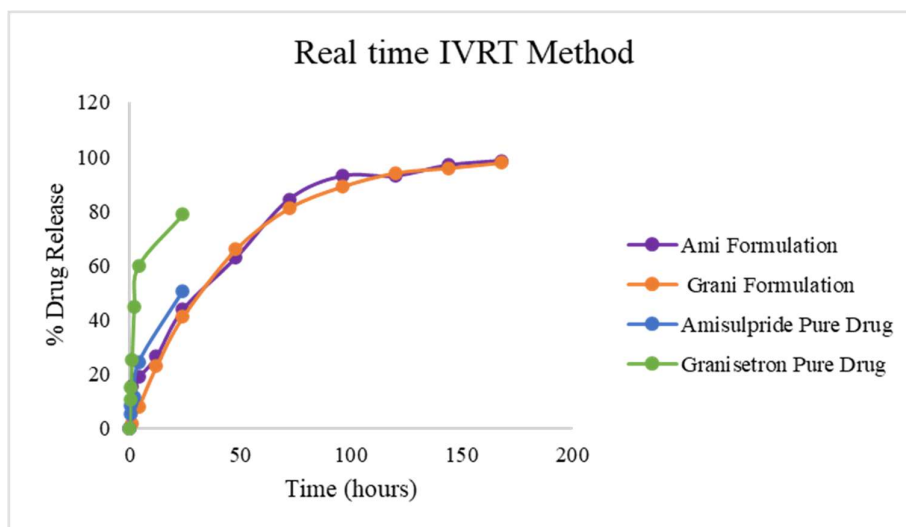
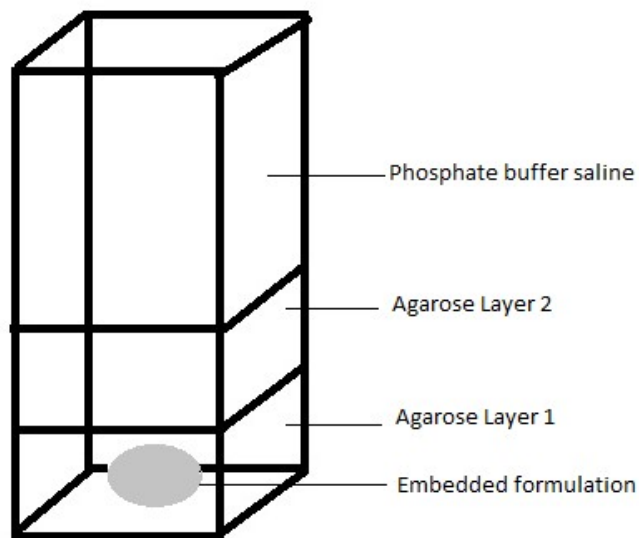


Figure 7-8 IVRT data from Real time *in-vitro* release testing method

The drug release using RT method showed that, around 40-50% drug was released at 24-hour and almost complete release was observed at 168-hour. This showed that, the drug release at 4 hour and 24 hours in ACC method is correlating with drug release at 24 hour and 168 hours in real time method. This was helpful in the way that, the formulation behaviour can be understood from ACC release method without need to wait for 168 hours for complete release.

### C) Development of *In-vitro* Gel Diffusion Model:

After intramuscular or subcutaneous injection, the formulation comes in vicinity of extracellular matrix made up of a fibrous polymer framework of collagen and hyaluronic acid. This matrix simulates a gel like scenario instead of bulk fluid, due to which mass transport and diffusion of the drug are significantly affected thereby changing overall absorption profile of the drug. The bio performance of a formulation administered using subcutaneous/intramuscular route can be understood by simulating these conditions. Agarose in water form a three-dimensional structure similar to *in-vivo* environment. Hence, the drug movement through this system may provide more biorelevant conditions for formulations. 1% Agarose gel was prepared by the method mentioned by Leung et al. [15] Briefly, 100 mg agarose was suspended in 10 ml of phosphate buffer pH 7.4 and heated to 80°C till clear solution obtained. Then it was cooled to 60°C. 1-2 mg of formulation was introduced at the bottom of cuvette and filled with agarose solution. Gently mixing of sample and gel was performed to achieve uniformity. Then the cuvette was kept at 5°C for 5 min to settle the gel. Another layer of agarose gel was added and further cooled at 5°C for 5 min. Lastly, 3 ml of PBS was added. The graphical presentation is shown in figure 7-9.

Figure 7-9 *In-vitro* gel diffusion system setup

Drug released in the PBS was measured periodically up to 24 hours by UV-visible spectrophotometer at respective drug wavelengths. This method simulates *in-vivo* drug release mechanism and conditions after intramuscular/subcutaneous administration.

The results are shown in figure 7-10, table 7-8 and table 7-9. % RSD has been mentioned in bracket.

Table 7-8 Gel diffusion *in-vitro* release testing method (Pure drug)

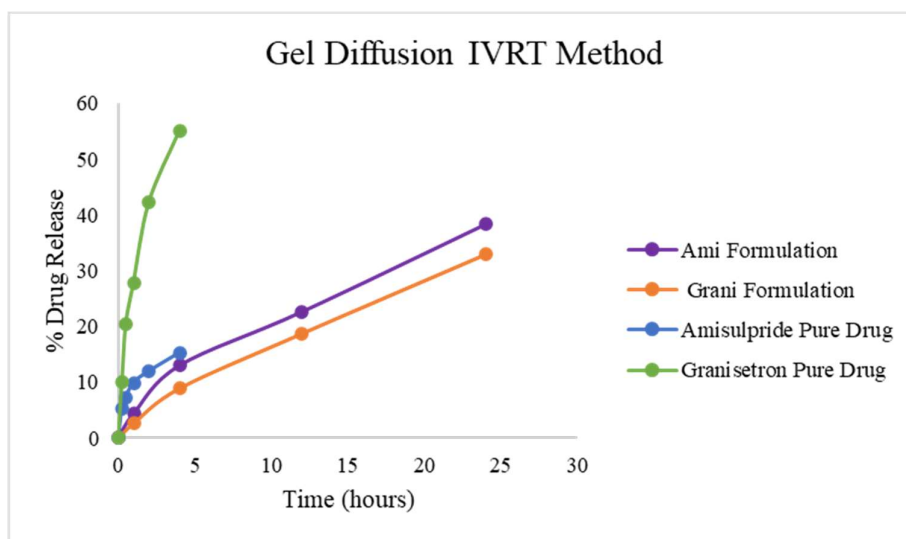
Gel diffusion <i>in-vitro</i> release testing method		
Time (hours)	Ami Pure Drug	Grani Pure Drug
0	0	0
0.25	5.3 (22.01)	10.1 (14.94)
0.5	7.3 (14.43)	20.4 (9.82)
1	9.9 (13.96)	27.8 (8.72)
2	12.0 (10.58)	42.2 (7.94)
4	15.3 (10.51)	55.1 (4.65)
24	18.3 (10.12)	64.7 (3.40)

Note: % RSD values provided for mean values in bracket

Table 7-9 Drug release as per Gel Diffusion IVRT method (Formulation)

Gel diffusion <i>in-vitro</i> release testing method		
Time (hours)	Ami	Grani
0	0	0
1	4.3 (18.51)	2.6 (30.04)
4	13.0 (10.97)	8.9 (17.66)
12	22.7 (9.71)	18.7 (8.61)
24	38.4 (4.99)	32.9 (5.02)

Note: % RSD values provided for mean values in bracket

Figure 7-10 IVRT data from Gel diffusion *in-vitro* release testing method

Drug release in the gel diffusion method was slow compared to ACC and real time method due to the presence of gel mimicking muscle or subcutaneous tissues.

#### 7.2.10 *In-vitro* Drug release kinetics:

*In-vitro* drug release kinetics from Janus microspheres was determined using methods mentioned in table 7-10. The drug release kinetics data for optimized formulations is shown in table 7-11 and 7-12.

Table 7-10 Drug release kinetics

Sr. No.	Drug release model	Model equation and details	Reference No.
1	Zero order	$F = k_0 x t$	16
2	First order	$F = 100 x [1 - e^{-k_1 t}]$	17,18
3	Higuchi	$F = kH x t^{0.5}$	19, 20
4	Korsmeyer - Peppas	$F = kKp x t^n$ , <i>n = 0.5 is fickian diffusion</i> <i>0.5 &lt; n &lt; 1.0 is no – fickian transport</i> <i>n = 1.0 is zero order kinetics</i> <i>n &gt; 1.0 is super case II transport</i>	21-23
5	Hixon Crowell	$F = 100 x [1 - (1 - KHC x t)^3]$	24,25
6	Weibull	$F = 100 x [1 - e^{-(t^\beta)/\alpha}]$	26

Three different methods were developed with different objectives.

The accelerated method was developed for quality control purpose, as long duration of real time and gel diffusion methods was not practically feasible for optimizing the formulations. Real time method mimics the drug release for the designated treatment duration that is 7 days. Gel diffusion method was developed with the objective of establishing bio relevancy to the muscle tissue environment.

Good correlation was observed between accelerated and real time methods, hence accelerated method was used for optimizing the formulation which provided the formulation behaviour in relatively shorter time period.

Out of these three methods, we have developed IVIVC with real time method as it did not required time scaling to match in-vivo time points.

Table 7-11 Mathematical model details for ACC IVRT method

ACC Ami Formulation						
Model	R2	K	AIC	n	$\alpha$	$\beta$
Zero order	0.4616	4.528	31.3			
First order	0.8418	0.125	26.41			
<b>Higuchi</b>	<b>0.9587</b>	<b>20.068</b>	<b>21.04</b>			
<b>Korsmeyer-Peppas</b>	<b>0.9759</b>	<b>24.528</b>	<b>20.88</b>	<b>0.425</b>		
Hixson-Crowell	0.7835	0.032	27.66			
Weibull	0.929		25.2		4.003	0.674
ACC Grani Formulation						
Model	R2	K	AIC	n	$\alpha$	$\beta$
Zero order	0.6495	4.528	30.16			
First order	0.9274	0.118	23.86			
<b>Higuchi</b>	<b>0.9938</b>	<b>19.896</b>	<b>14.048</b>			
<b>Korsmeyer-Peppas</b>	<b>0.9947</b>	<b>21.007</b>	<b>15.35</b>	<b>0.48</b>		
Hixson-Crowell	0.8795	0.31	25.24			
Weibull	0.958		23.67		5.211	0.776

Table 7-12 Mathematical model details for RT IVRT method

RT Ami Formulation						
Model	R2	K	AIC	n	$\alpha$	$\beta$
Zero order	0.5794	0.758	85.92			
First order	0.9686	0.024	59.96			
Higuchi	0.955	8.548	63.578			
<b>Korsmeyer-Peppas</b>	<b>0.9687</b>	<b>12.251</b>	<b>61.96</b>	<b>0.422</b>		
Hixson-Crowell	0.9578	0.007	62.919			
<b>Weibull</b>	<b>0.9735</b>		<b>60.273</b>		<b>24.269</b>	<b>0.864</b>
RT Grani Formulation						
Model	R2	K	AIC	n	$\alpha$	$\beta$
Zero order	0.7223	0.748	83.92			
<b>First order</b>	<b>0.9998</b>	<b>0.023</b>	<b>12.58</b>			
Higuchi	0.9615	8.37	64.16			
Korsmeyer-Peppas	0.9617	8.763	66.11	0.49		
Hixson-Crowell	0.9945	0.006	44.78			
<b>Weibull</b>	<b>1</b>		<b>9.832</b>		<b>49.771</b>	<b>1.03</b>

**7.2.11 Results and Discussion of IVRT data:**

Three types of *in-vitro* drug release methods were developed to gain understanding of mechanism of drug release under different conditions. The sustained drug release from polymeric microspheres have been attributed to delayed degradation of the polymer matrix [14]. The accelerated method employs elevated temperatures which resulted in increased rate of matrix degradation and drug diffusion across the matrix [27]. The results from all three methods were suggestive of drug releasing slowly through matrix and thus providing sustained action over a specified period of time. The drug release of Amisulpride was best fitted with Korsmeyer-Peppas equation with  $R^2$  close to 0.9. The release of Granisetron followed first order kinetics with  $R^2$  close to 0.9 in real time drug release method.

Weibull model fitting was performed for optimized formulations for *in-vivo* simulations.

**7.2.12 Stability of Formulations:**

The optimized formulations were tested for stability at 2-8°C for 6 months and 25°C/60% RH for 3 months in stoppered and sealed 10 ml USP-type I glass vials. The stability study was performed to evaluate the impact of storage conditions on assay and particle size of formulations. The results in Table 7-13 indicate that formulations were stable up to 6 months at 2-8°C and 3 months at 25°C/60% RH. No significant changes were observed for the tested parameters.

Table 7-13 Stability studies of Optimized Formulation

Storage conditions	Interval (M)	% Assay of Amisulpride	% Assay of Granisetron	Particle size (D90) in ( $\mu\text{m}$ )	Sterility testing as per USP
Initial	0	99.90 $\pm$ 0.56	100.03 $\pm$ 0.68	91.753 $\pm$ 4.02	Pass
2-8°C	3	98.27 $\pm$ 0.95	98.67 $\pm$ 0.57	92.601 $\pm$ 4.19	Pass
	6	98.17 $\pm$ 0.76	98.63 $\pm$ 0.45	93.509 $\pm$ 7.01	Pass
25°C/60% RH	1	98.20 $\pm$ 1.00	98.07 $\pm$ 1.21	92.706 $\pm$ 6.68	Not done
	2	97.80 $\pm$ 1.57	98.00 $\pm$ 0.72	92.108 $\pm$ 3.32	Not done
	3	97.50 $\pm$ 1.76	96.87 $\pm$ 0.58	92.362 $\pm$ 5.18	Pass
<i>Note: <math>\pm</math> SD values provided for mean values</i>					

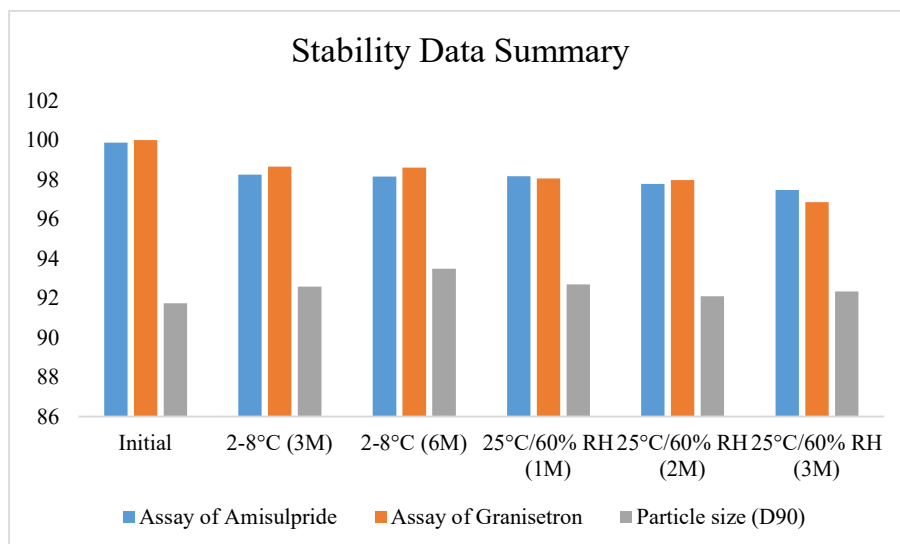


Figure 7-11 Stability data Trend at studied stations

From trend analysis, it was concluded that optimized formulations are stable and showed consistent results throughout the stability studies.

### 7.2.13 Bio-interactions of prepared formulations:

#### Haemolysis study

Haemolysis study was performed by slight modification of method mentioned by Ritu K et.al [28]. Briefly, for this study, 1.0 ml blood was taken from the Sprague Dawley rat by retro-orbital puncture in an Eppendorf tube containing Ethylene diamine tetracetic acid (EDTA) solution (30  $\mu$ l). Centrifugation of sample done in 5  $^{\circ}$ C at 6000 rpm for 10 min for separation of erythrocytes. Plasma components were removed by repetitive washing of residue after centrifugation with normal saline. Amisulpride + granisetron suspension and formulation along with prepared RBC with saline was used for measurement. 1 ml of 2.0% Triton-X100 was used as positive control and 0.5% dimethyl sulfoxide (DMSO) was used as negative control. After treatment, the dispersions were stored at 37 $^{\circ}$ C for 20 min in incubator. After incubation, all the samples were separated from mass of RBCs by centrifugation as earlier and then analyzed at  $\lambda_{max}$  of 540 nm against normal saline as a reference solution [29,30] Haemolysis % was estimated using following equation 7-2:

$$\% \text{ Haemolysis} = \frac{A_{540} \text{ of sample} - A_{540} \text{ of negative control}}{A_{540} \text{ of positive control} - A_{540} \text{ of negative control}} \times 100 \text{ ----- equation 7-2}$$

The absorbance for positive control (Triton X- 100) and negative control (DMSO) was found to be 0.70 and 0.150 respectively. The % haemolysis for optimized formulation was found to be 1.3 %  $\pm$  0.05 %. The results demonstrated no significant haemolysis potential of optimized formulation as the % haemolysis was found to be less than 2 [28].

### 7.3 In-silico evaluation

The in-silico evaluation of optimized formulation was performed using developed PBPK model (Refer Chapter 3 section 3.2 In-silico model development).

#### 7.3.1 Prediction of *In-vivo* pharmacokinetics:

Developed PBPK model using intravenous data and verified with single and multiple dose oral formulations data was used to predict the *in-vivo* performance of sustained release once weekly formulations.

Initially, the drug release data from calculated dissolution models was used to build preliminary PBPK model for sustained release formulations after intramuscular administrations. This was required to set physiological parameters which account for behaviour of drug after intramuscular administration. After initial model refinement, actual drug release data was used to predict the *in-vivo* pharmacokinetics of sustained release formulations. The optimized once a weekly formulation showed comparable *in-vivo* profile to that of multiple dose (MDD) profile (Figure 7-12 and 7-13)

The pharmacokinetics of antiemetic drugs (both amisulpride and granisetron) is directly predictive of their pharmacodynamics. The details are presented in figure 7-12 and 7-13.

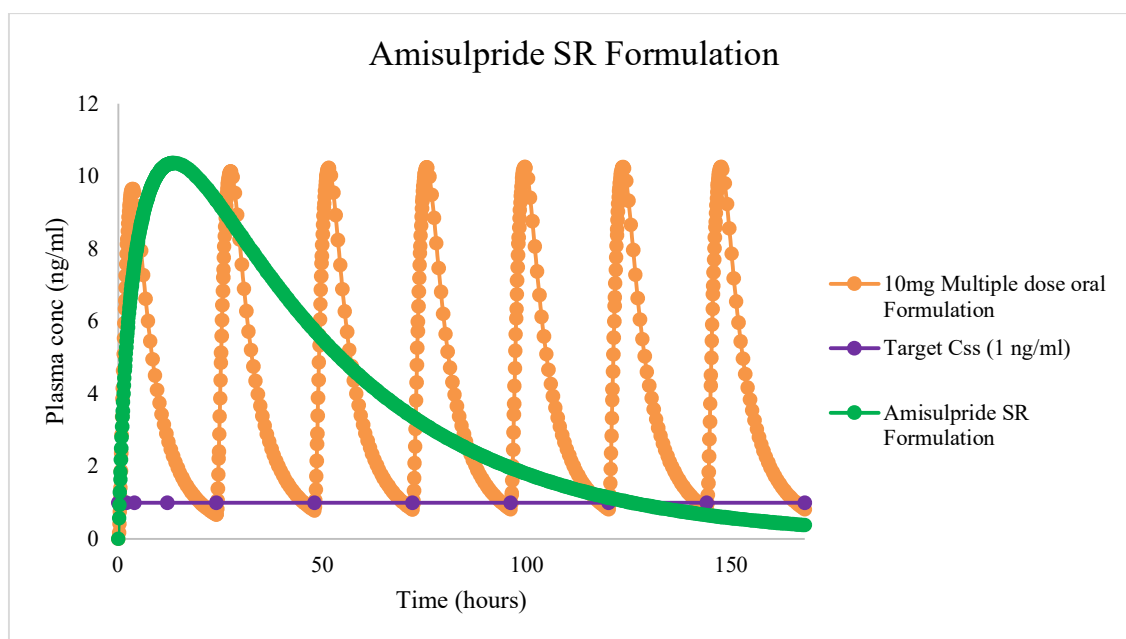


Figure 7-12 Prediction of *in-vivo* PK for once a weekly formulation of Amisulpride

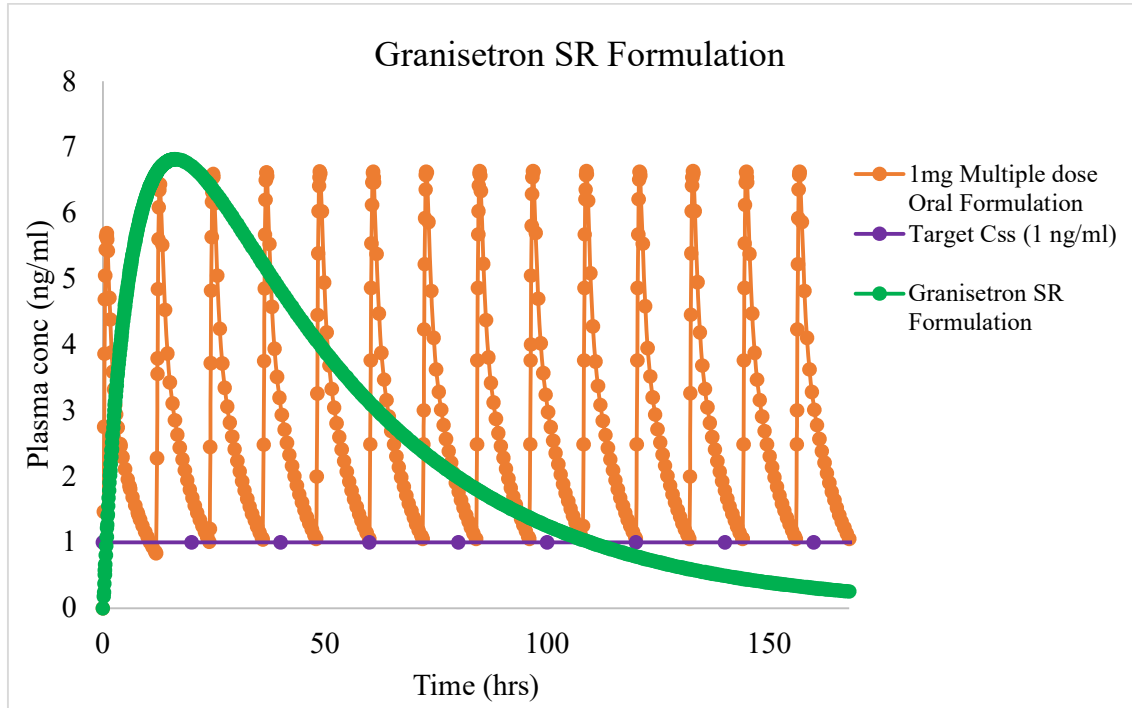


Figure 7-13 Prediction of *in-vivo* PK for once a weekly formulation of Granisetron

### 7.3.2 Virtual bioequivalence studies:

Virtual bioequivalence (VBE) studies were conducted in healthy subjects between optimized test formulation and reference multiple dose formulation to assess the *in-vivo* pharmacokinetic bioequivalence. These trials were designed taking account the regulatory requirements of *in-vivo* pharmacokinetic bioequivalence studies as such study design, treatments, dosing, number of subjects to attain sufficient power and statistical analysis methodology. The summary of results is shown in Figure 7-14 and Figure 7-15.

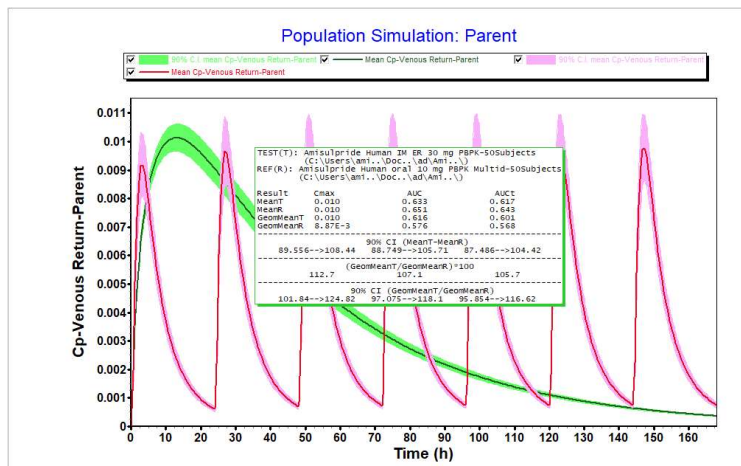


Figure 7-14 Virtual bioequivalence of once a weekly formulation of Amisulpride (30 mg) against oral 10 mg multiple dosing

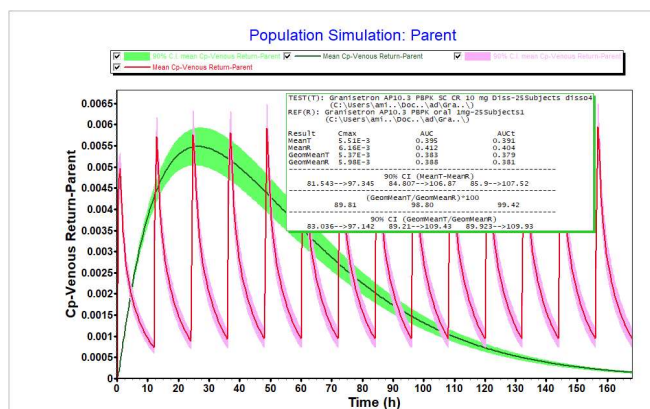


Figure 7-15 Virtual bioequivalence of once a weekly formulation of Granisetron (10 mg) against oral 1 mg multiple dosing

Gastroplus population bioequivalence feature allows user to incorporate all these factors while running the virtual bioequivalence studies. The inherent variabilities between the subjects such as body weight, age, male to female ratio, physiological variations were all integrated while running these simulations. The VBE results confirmed that the developed once a weekly formulation achieved similar rate (Cmax) and extent (AUC) as that of immediate release multiple dose formulations and both developed SR formulation and multiple dose IR formulations are bioequivalent to each other (Refer caption in Figure 7-14 and 7-15). Thus, the same efficacy was achieved by the developed sustained release formulation as that of multiple dose immediate release formulation by reducing frequent fluctuations that arise due to repeated dosing. This formulation also provided patient compliance due to once weekly administration.

### 7.3.3 Predictive IVIVC to establish design space:

*In-vitro in-vivo* correlation was developed for slow, medium and fast release formulations. Formulations with different drug: polymer ratio resulted in different release rates, which were used in developing the IVIVC. The details are provided in Table 7-14 and figure 7-16A and 7-16B. Advanced compartmental and transit (ACAT) model was used to mechanistically predict the *in-vivo* drug release profiles of three different release rate formulations (Table 7-14). The interpolation function was used to build the correlation. Power correlation function was found best suitable with highest R2 value. The convolution results of all three formulations showed, both individual and mean Absolute Percent Prediction Errors well within the limits of NMT 15% and 10% respectively. The details are presented in Table 7-15 & 7-16 and Figure 7-17 & 7-18 for amisulpride and granisetron respectively. Real time method did not require time scaling to match *in-vivo* time points and also successfully showed excellent rank order for different release rate formulations, which resulted in best IVIVC.

Table 7-14 Drug release of formulations used in building IVIVC

Time in (hours)	Amisulpride			Granisetron		
	Slow (D:P = 0.1)	Medium (D:P = 0.4)	Fast (D:P = 0.6)	Slow (D:P = 0.1)	Medium (D:P = 0.4)	Fast (D:P = 0.6)
0	0	0	0	0	0	0
1	3.1 (17.1)	10.2 (12.8)	20.1 (9.9)	1.3 (23.1)	2.1 (16.5)	6.2 (17.4)
4	7.2 (6.9)	12.9 (8.2)	23.2 (8.0)	4.4 (15.9)	7.9 (13.4)	16.4 (7.6)
24	35.8 (4.9)	40.5 (4.1)	46.8 (2.4)	29.8 (3.9)	40.9 (5.0)	52.2 (4.9)
168	99.1 (1.0)	99.0 (0.4)	99.1 (0.8)	98.8 (0.6)	99.0 (0.8)	98.7 (1.3)

Note: % RSD values provided for mean values in bracket

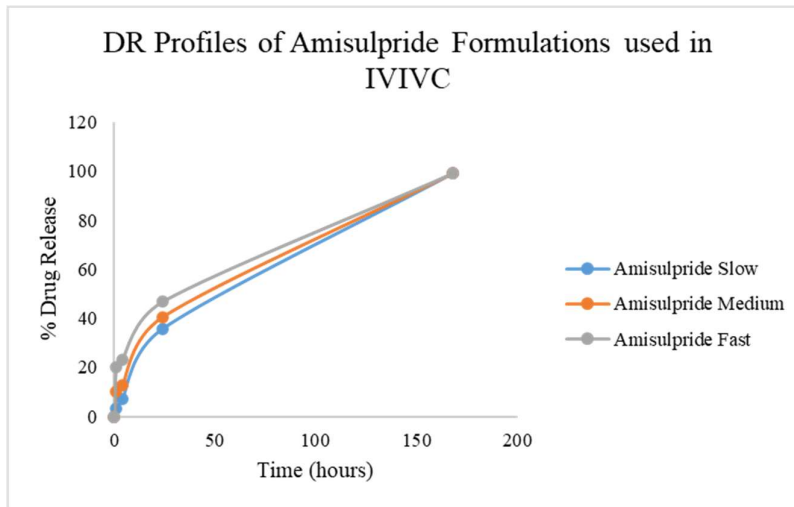


Figure 7-16A *In-vitro* drug release profiles of Amisulpride formulations with different release rates in real time method

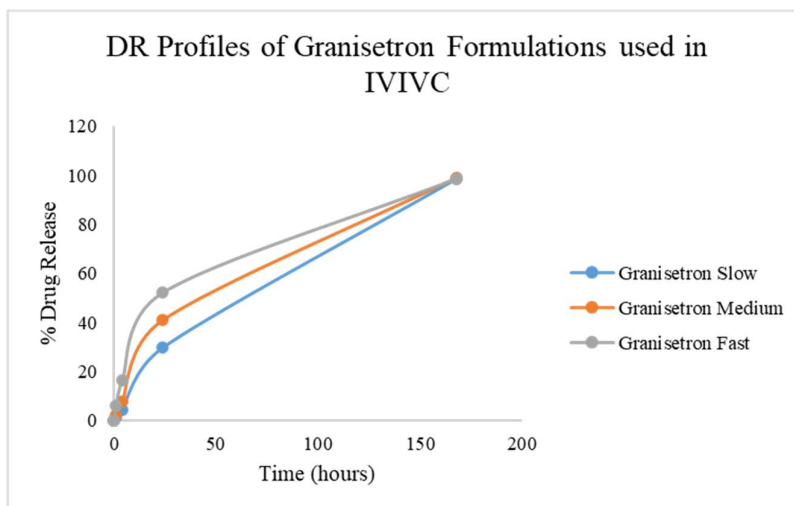


Figure 7-16B *In-vitro* drug release profiles of Granisetron formulations with different release rates in real time method

Table 7-15 IVIVC Details for Amisulpride

Validation Statistics for Amisulpride IVIVC						
Drug Record	Cmax (ng/mL)			AUCt (ng/mL*h)		
	Obs.	Pred.	% Pred. Error	Obs.	Pred.	% Pred. Error
Amisulpride 30 mg CR Slow	9.11	9.127	-0.187	620.1	632.8	-2.05
Amisulpride 30 mg CR Medium	10.32	10.41	-0.883	626.8	632.3	-0.876
Amisulpride 30 mg CR Fast	13.97	14.37	-2.887	618.5	621.1	-0.411
Mean Absolute Percent Prediction Error	1.319			1.112		
$y = 0.997 * (x)^{0.992}$						
where x=Fraction released <i>in-vitro</i> and y=Fraction released <i>in-vivo</i>						
Correlation = Power Function						
Statistics for Reconstructed Plasma Concentration-Time Profile from Convolution Tab						
Drug Record	R <sup>2</sup>	SEP	MAE	AIC		
Amisulpride 30 mg CR Slow	1	0.038	0.02	-43.32		
Amisulpride 30 mg CR Medium	1	0.049	0.026	-37.93		
Amisulpride 30 mg CR Fast	1	0.078	0.039	-27.83		

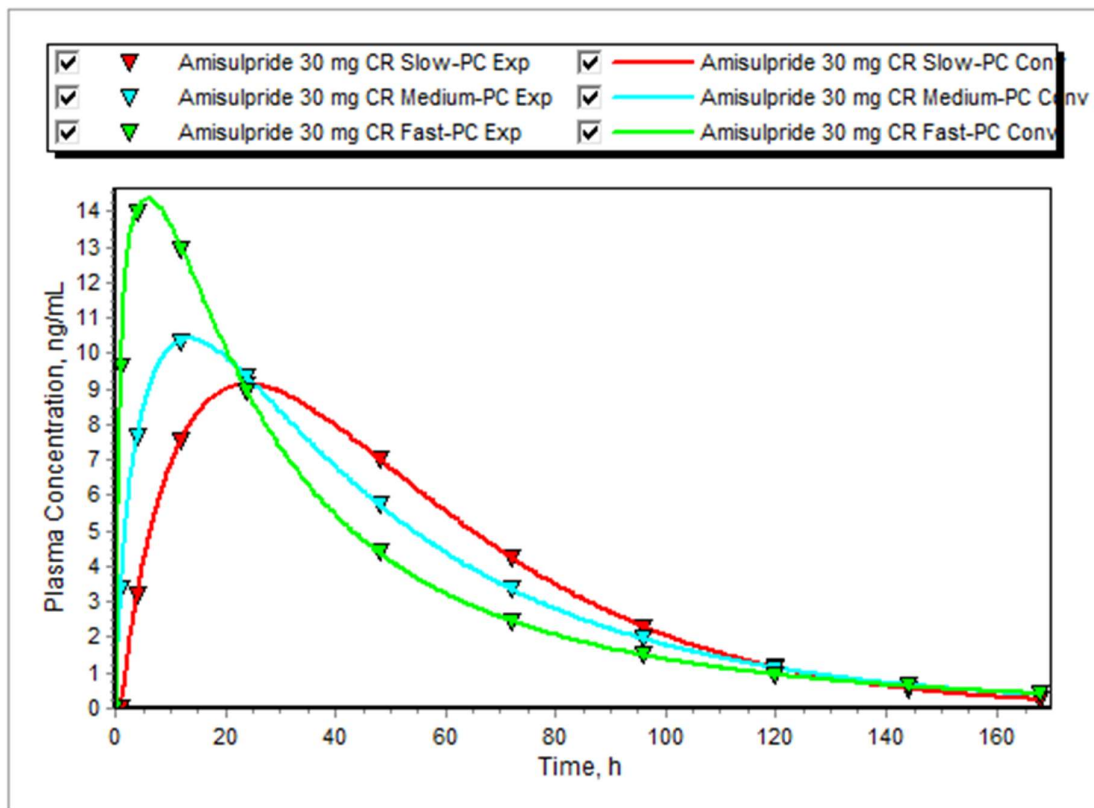


Figure 7-17 IVIVC predictions for Amisulpride

Table 7-16 IVIVC Details for Granisetron

Validation Statistics for Granisetron						
Drug Record	Cmax (ng/mL)			AUCt (ng/mL*h)		
	Obs.	Pred.	% Pred. Error	Obs.	Pred.	% Pred. Error
Granisetron CR 10 mg Slow	5.962	5.41	9.25	416.5	410.4	1.468
Granisetron CR 10 mg medium	6.598	6.579	0.286	422.9	416.5	1.519
Granisetron CR 10 mg fast	8.684	8.726	-0.484	423.8	407.8	3.772
Mean Absolute Percent Prediction Error	3.34			2.253		
$y = 0.999x^{1.033}$						
where x=Fraction released <i>in-vitro</i> and y=Fraction released <i>in-vivo</i>						
Correlation = Power Function						
Statistics for Reconstructed Plasma Concentration-Time Profile from Convolution Tab						
Drug Record	R <sup>2</sup>	SEP	MAE	AIC		
Granisetron CR 10 mg Slow	0.986	0.241	0.174	-2.934		
Granisetron CR 10 mg medium	0.997	0.116	0.081	-18.95		
Granisetron CR 10 mg fast	0.993	0.247	0.167	-2.381		

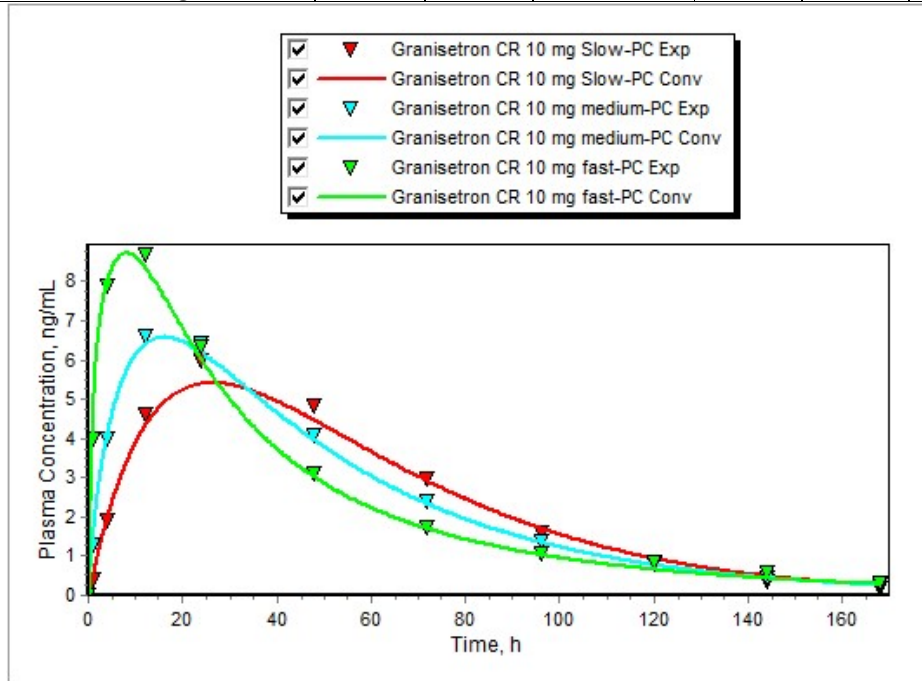


Figure 7-18 IVIVC predictions for Granisetron

Table 7-15 and Table 7-16 show the IVIVC details. The % prediction error less than 15% suggests that IVIVC meets the USFDA regulatory acceptance criteria. The standard error of prediction (SEP), mean absolute error (MAE) and Akaike information criteria (AIC) are the statistical parameters that show the capability of IVIVC model.

### 7.4 References:

1. Singh, Gurpreet & Tanurajvir, Kaur & Ravinder, Kaur & Kaur, Anudeep. (2014). Recent biomedical applications and patents on biodegradable polymer-PLGA. *International Journal of Pharmacology and Pharmaceutical Sciences*. 1. 30-42.
2. Gökalp, Nurefşan & Ulker Turan, Cansu & Guvenilir, Yuksel. (2016). Synthesis of Polycaprolactone via Ring Opening Polymerization Catalyzed by *Candida Antarctica* Lipase B Immobilized onto an Amorphous Silica Support. *Journal of Polymer Materials*. 33. 87-100.
3. <https://pubchem.ncbi.nlm.nih.gov/compound/Amisulpride>
4. Evren Algin Yapar et. al Thermal analysis on phase sensitive granisetron in situ forming implants *Journal of Applied Pharmaceutical Science* Vol. 4 (07), pp. 010-013, July, 2014
5. Kapoor, Deepak & Bhatia, Amit & Kaur, Ripandeep & Sharma, Ruchi & Kaur, Gurvinder & Dhawan, Sanju. (2015). PLGA: A unique polymer for drug delivery. *Therapeutic delivery*. 6. 41-58. 10.4155/tde.14.91.
6. González-González AM et.al In Vitro and In Vivo Evaluation of a Polycaprolactone (PCL)/Polylactic-Co-Glycolic Acid (PLGA) (80:20) Scaffold for Improved Treatment of Chondral (Cartilage) Injuries. *Polymers (Basel)*. 2023 May 16;15(10):2324.
7. Patent CN109718225B Granisetron slow release microspheres and preparation method thereof
8. Winkler JS, Barai M, Tomassone MS. Dual drug-loaded biodegradable Janus particles for simultaneous co-delivery of hydrophobic and hydrophilic compounds. *Exp Biol Med (Maywood)*. 2019 Oct;244(14):1162-1177.
9. Mao S, Xu J, Cai C, Germershaus O, Schaper A, Kissel T. Effect of WOW process parameters on morphology and burst release of FITC-dextran loaded PLGA microspheres. *International journal of pharmaceutics*. 2007 Apr 4;334(1-2):137-48.
10. United states pharmacopoeia, Edition 31, Chapter 1174, Flow Properties
11. Yang Z, Liu L, Su L, Wu X, Wang Y, Liu L, Lin X. Design of a zero-order sustained release PLGA microspheres for palonosetron hydrochloride with high encapsulation efficiency. *Int J Pharm*. 2020 Feb 15;575:119006.
12. Zixu Liu, Ruixuan Bu, Linxuan Zhao, Lei Liu, Nan Dong, Yu Zhang, Tian Yin, Haibing He, Jingxin Gou, Xing Tang, Hydrogel-containing PLGA microspheres of palonosetron hydrochloride for achieving dual-depot sustained release, *Journal of Drug Delivery Science and Technology*, Volume 65,2021, 102775.

13. Sinha VR, Trehan A. Formulation, characterization, and evaluation of ketorolac tromethamine-loaded biodegradable microspheres. *Drug Deliv.* 2005 May-Jun;12(3):133-9.
14. Dabke A, Ghosh S, Dabke P, Sawant K, Khopade A. Revisiting the *in-vitro* and *in-vivo* considerations for in-silico modelling of complex injectable drug products. *J Control Release.* 2023 Aug;360:185-211.
15. Leung DH, Kapoor Y, Alleyne C, Walsh E, Leithead A, Habulihaz B, Salituro GM, Bak A, Rhodes T. Development of a Convenient In Vitro Gel Diffusion Model for Predicting the In Vivo Performance of Subcutaneous Parenteral Formulations of Large and Small Molecules. *AAPS PharmSciTech.* 2017 Aug;18(6):2203-2213.
16. Brooke D, Washkuhn RJ. Zero-order drug delivery system: theory and preliminary testing. *Journal of pharmaceutical sciences.* 1977 Feb 1;66(2):159-62.
17. Levy G, Hollister LE. Inter-and intrasubject variations in drug absorption kinetics. *Journal of Pharmaceutical Sciences.* 1964 Dec 1;53(12):1446-52.
18. Gibaldi M, Feldman S. Establishment of sink conditions in dissolution rate determinations. Theoretical considerations and application to nondisintegrating dosage forms[J]. *J Pharm Sci*, 1967, 56(10): 1238-1242.
19. Higuchi T. Rate of release of medicaments from ointment bases containing drugs in suspension. *Journal of pharmaceutical sciences.* 1961 Oct 1;50(10):874-5.
20. Higuchi WI. Diffusional models useful in biopharmaceutics: drug release rate processes. *Journal of pharmaceutical sciences.* 1967 Mar 1;56(3):315-24.
21. Korsmeyer RW, Gurny R, Doelker E, Buri P, Peppas NA. Mechanisms of solute release from porous hydrophilic polymers. *International journal of pharmaceutics.* 1983 May 1;15(1):25-35.
22. Peppas N A. Analysis of Fickian and non-Fickian drug release from polymers.[J]. *Pharm Acta Helv*, 1985, 60(4): 110-111.
23. Ritger PL, Peppas NA. A simple equation for description of solute release I. Fickian and non-fickian release from non-swelling devices in the form of slabs, spheres, cylinders or discs. *Journal of controlled release.* 1987 Jun 1;5(1):23-36.
24. Hixson A W, Crowell J H. Dependence of Reaction Velocity upon surface and Agitation[J]. *Industrial & Engineering Chemistry*, 1931, 23(8): 923-931.
25. Lu DR, Abu-Izza K, Mao F. Nonlinear data fitting for controlled release devices: an integrated computer program. *International journal of pharmaceutics.* 1996 Mar 8;129(1-2):243-51.

26. Sathe PM, Tsong Y, Shah VP. *In-vitro* dissolution profile comparison: statistics and analysis, model dependent approach. *Pharmaceutical research*. 1996 Dec;13:1799-803.
27. A. Mansuri, M. Völkel, T. Feuerbach, J. Winck, A.W. Vermeer, W. Hoheisel, et al., Modified free volume theory for self-diffusion of small molecules in amorphous polymers, *Macromolecules* 56 (8) (2023) 3224–3237.
28. Kudarha RR. Development of Nanocarrier Based Targeted Drug Delivery System for Effective Treatment of Brain Tumor (Doctoral dissertation, Maharaja Sayajirao University of Baroda (India)).
29. Zhang G-S, Hu P-Y, Li D-X, He M-Z, Rao X-Y, Luo X-J, et al. Formulations, Hemolytic and Pharmacokinetic Studies on Saikosaponin a and Saikosaponin d Compound Liposomes. *Molecules*. 2015 Apr;20(4):5889–907.
30. Yadav AK, Agarwal A, Rai G, Mishra P, Jain S, Mishra AK, et al. Development and characterization of hyaluronic acid decorated PLGA nanoparticles for delivery of 5-fluorouracil. *Drug Deliv*. 2010 Nov;17(8):561–72.